Reversion-induced LIM interaction with Src reveals a novel Src inactivation cycle

Yongjun Zhang, Yizeng Tu, Jianping Zhao, Ka Chen, and Chuanyue Wu

Department of Pathology, University of Pittsburgh, Pittsburgh, PA 15261

Aberrant Src activation plays prominent roles in cancer progression. However, how Src is activated in cancer cells is largely unknown. Genetic Src-activating mutations are rare and, therefore, are insufficient to account for Src activation commonly found in human cancers. In this study, we show that reversion-induced LIM (RIL), which is frequently lost in colon and other cancers as a result of epigenetic silencing, suppresses Src activation. Mechanistically, RIL suppresses Src activation through interacting with Src and PTPL1, allowing PTPL1-dependent dephosphorylation of Src at the activation loop. Importantly, the binding of RIL to Src is drastically reduced upon Src inactivation. Our results reveal a novel Src inactivation cycle in which RIL preferentially recognizes active Src and facilitates PTPL1-mediated inactivation of Src. Inactivation of Src, in turn, promotes dissociation of RIL from Src, allowing the initiation of a new Src inactivation cycle. Epigenetic silencing of *RIL* breaks this Src inactivation cycle and thereby contributes to aberrant Src activation in human cancers.

Introduction

Src is an important regulatory protein that functions in several fundamental processes, including cell differentiation, proliferation, migration, and survival (Summy and Gallick, 2003, 2006; Frame, 2004; Playford and Schaller, 2004; Russello and Shore, 2004; Yeatman, 2004). Because of its prominent roles in cell signaling, aberrant Src activation, which is frequently found in common human cancers such as colon cancer (Rosen et al., 1986; Bolen et al., 1987; Cartwright et al., 1989, 1990; Aligayer et al., 2002), is considered a key factor in cancer progression. Thus, inhibition of Src represents a promising approach for cancer therapy. Indeed, a large number (>50 at last count) of Src inhibitor–based clinical trials have been initiated (Kopetz et al., 2007). However, despite the wealth of information on the structural basis and functional consequences of Src activation (Thomas and Brugge, 1997), how Src is activated in cancer cells remains largely elusive.

Reversion-induced LIM (RIL) is a ubiquitously expressed protein that was initially identified during a search for genes that are expressed in normal cells but repressed in Harvey ras–transformed derivatives (Kiess et al., 1995). The expression of *RIL* is restored in several independent phenotypic revertants derived from Harvey ras–transformed cells (thus, it was named as reversion-induced LIM). Recent experiments have shown that *RIL* is a target of epigenetic silencing (Boumber et al., 2007). Hypermethylation of *RIL* was found in a large number of cancer cell lines and tumors derived from various origins, including the colon, liver, and breast (Boumber et al., 2007). Furthermore, *RIL* transcription is suppressed in multiple types of human cancer cells, including colon cancer cells, and reexpression of RIL inhibited anchorage-independent growth (Boumber et al., 2007). These findings strongly suggest that loss of RIL contributes to malignant behavior. However, the underlying molecular mechanism is not known. In this study, we show that RIL mediates a novel Src inactivation cycle and, thus, that loss of RIL promotes Src activation and consequently anchorage-independent growth.

Results and discussion

We first verified that the expression of RIL protein was inhibited in human colon cancer cells. To do this, we generated an mAb specifically recognizing RIL. Western blotting analyses of HCT116 (Fig. 1 A, lane 2), HT29 (Fig. 1 A, lane 3), RKO (Fig. 1 A, lane 4), Caco-2 (Fig. 1 A, lane 5), and DLD-1 (Fig. 1 A, lane 6) colon cancer cells showed that they all lacked RIL. Additionally, no RIL was detected in several other types of cancer

Correspondence to Chuanyue Wu: carywu@pitt.edu

Abbreviations used in this paper: BL, BAS-like; MBP, maltose-binding protein; PTP, protein Tyr phosphatase; RIL, reversion-induced LIM.

The Rockefeller University Press $30.00
J. Cell Biol. Vol. 184 No. 6 785–792
www.jcb.org/cgi/doi/10.1083/jcb.200810155

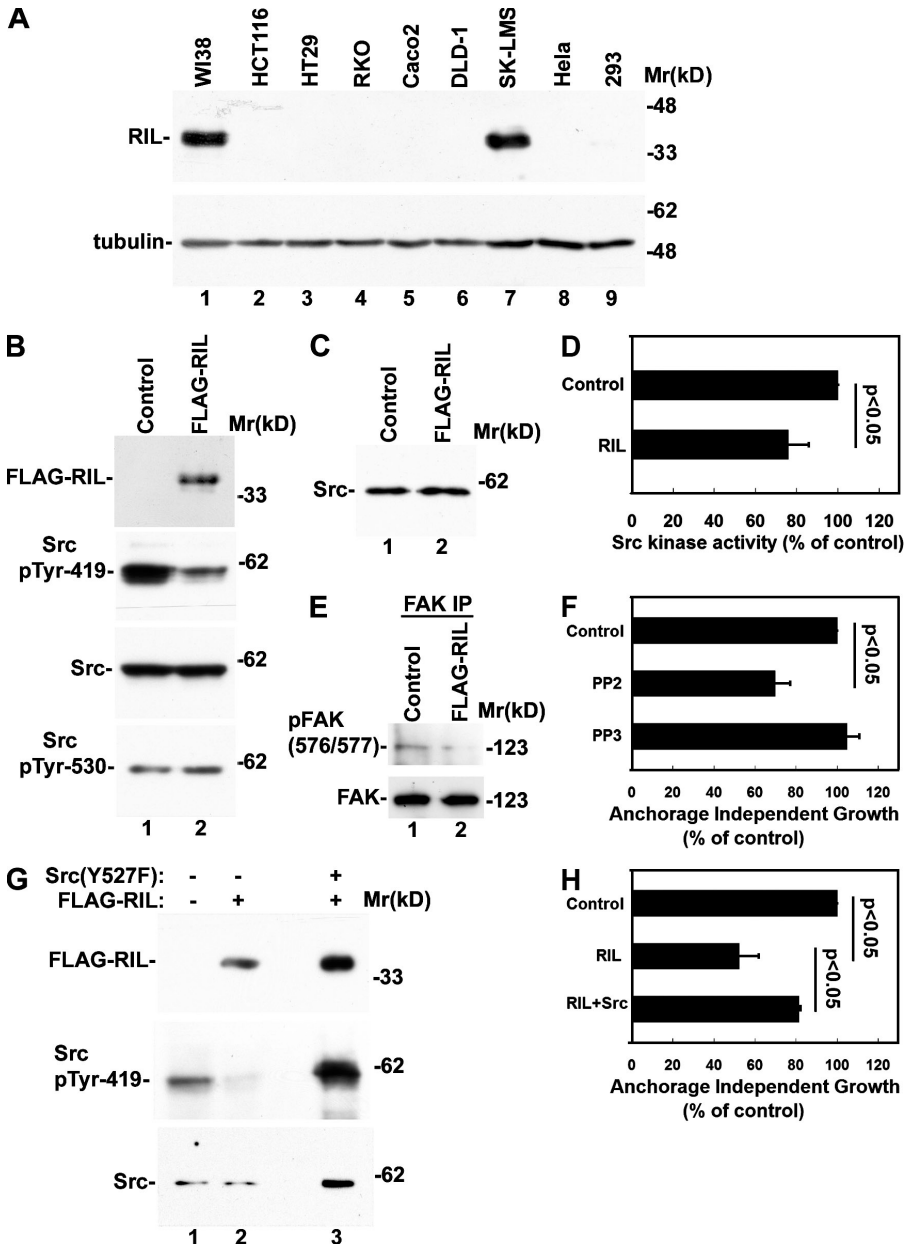

Figure 1. **RIL inhibits Src activation and reduces anchorage-independent growth.** (A) Lysates (15 µg/lane) of WI-38 (lane 1), HCT116 (lane 2), HT29 (lane 3), RKO (lane 4), Caco-2 (lane 5), DLD-1 (lane 6), SK-LMS-1 (lane 7), HeLa (lane 8), and 293 (lane 9) cells were analyzed by Western blotting with antibodies recognizing RIL or tubulin (as a loading control). (B) HCT116 cells were transfected with Flag-RIL vector (lane 2) or a vector lacking the RIL sequence as a control (lane 1). The lysates were probed with antibodies recognizing RIL, Src, pY419 Src, or pY530 Src. (C) Src was immunoprecipitated from HCT116 cells transfected with the control (lane 1) or Flag-RIL (lane 2) vector and analyzed by Western blotting with an anti-Src antibody. (D) The kinase activity of Src derived from the Flag-RIL transfectants was compared with that of the control cells. (E) FAK was immunoprecipitated from HCT116 cells transfected with the control (lane 1) or Flag-RIL (lane 2) vector and analyzed by Western blotting with antibodies specific for FAK or pY566/577 FAK. IP, immunoprecipitation. (F) Anchorage-independent growth of HCT116 cells in the presence of PP2 or PP3 was compared with that of HCT116 cells grown in the absence of PP2 and PP3 (control). (G and H) HCT116 cells were transfected with the control vector (G, lane 1), the Flag-RIL vector (G, lane 2), or the Flag-RIL vector and a vector encoding a constitutively active form of chicken Src (Y527F; G, lane 3). (G) The lysates were probed with antibodies recognizing RIL, pY419 Src, or Src. (H) Anchorage-independent growth of the cells expressing Flag-RIL or Flag-RIL and constitutively active Src was compared with that of the control cells. (D, F, and H) Error bars represent mean ± SD (n = 3). Mr, molecular mass.

cells, including HeLa (Fig. 1 A, lane 8) and 293 (Fig. 1 A, lane 9) cells. The lack of signals in the RIL Western blots was not the result of technical issues with the anti-RIL mAb or the samples, as RIL was readily detected in other cells (Fig. 1 A, lanes 1 and 7) and tubulin was detected in all samples (Fig. 1 A). Thus, consistent with the epigenetic experiments showing hypermethylation of *RIL* (Boumber et al., 2007), colon cancer cells lack RIL protein.

The finding that RIL expression is suppressed in human colon cancer cells, in which Src is known to be aberrantly activated, prompted us to test whether RIL plays a role in Src inactivation. To do this, we expressed RIL in human HCT116 colon cancer cells (Fig. 1 B, lane 2). Phosphorylation of Y419 (Y416 in chickens) in the activation loop, which is essential for full activation of Src (Roskoski, 2005), was markedly reduced (by 48.2 ± 20.1%; mean ± SD; n = 6; $P < 0.001$), whereas the level of Y530 (Y527 in chickens) phosphorylation, which inhibits Src activity (Roskoski, 2005), was slightly increased (by a mean of 7.6 ± 4.4%; mean ± SD; n = 3; $P = 0.038$) in response to RIL expression (Fig. 1 B). The level of total Src was not changed (Fig. 1 B). To directly test whether RIL inhibits Src activation, we immunoprecipitated Src from RIL-expressing (Fig. 1 C, lane 2) and RIL-null control (Fig. 1 C, lane 1) cells. Consistent with the suppression of Y419 phosphorylation, the activity of Src isolated from the RIL-expressing cells was significantly lower than that of RIL-null control cells (Fig. 1 D). To further test this, we analyzed Y576/577 phosphorylation of FAK, an in vivo substrate of Src, and found that it was substantially reduced in response to the expression of RIL (Fig. 1 E). Collectively, these results suggest that RIL plays an important role in the suppression of Y419 phosphorylation and consequently the inactivation of Src.

Src is known to play a role in the regulation of anchorage-independent growth (Summy and Gallick, 2003, 2006; Frame, 2004; Playford and Schaller, 2004; Russello and Shore, 2004; Yeatman, 2004). Consistent with this, treatment of HCT116 cells with the Src inhibitor PP2 but not with PP3 (a PP2 analogue lacking Src inhibitory activity) reduced anchorage-independent growth (Fig. 1 F). Expression of Flag-RIL, like treatment of cells with PP2, significantly reduced anchorage-independent growth (Fig. 1 H). Importantly, RIL-induced inhibition of anchorage-independent growth was substantially reversed (Fig. 1 H) in response to expression of a constitutively active Src (Fig. 1 G, lane 3), suggesting that RIL inhibits anchorage-independent growth at least partly through the suppression of Src activation.

Next, we sought to determine the mechanism by which RIL suppresses Src activation. A fraction of RIL colocalized with Src, particularly in the perinuclear areas (Fig. 2, A–C). Consistent with a role of RIL in Src inactivation, RIL was undetectable in areas where high concentrations of phospho-Y419 (pY419) Src (i.e., active Src) were present (Fig. 2, D–F). The finding that a fraction of Src colocalizes with RIL (Fig. 2, A–C) prompted us to test whether Src physically interacts with RIL. To do this, we generated a maltose-binding protein (MBP)–tagged Src protein and found that it was coprecipitated with GST-RIL (Fig. 2 G, lane 3) but not with GST (Fig. 2 G, lane 2). Probing the same samples with an anti-pY419 Src antibody revealed that pY419 Src was enriched in the GST-RIL precipitates. To further analyze the binding, we generated GST-tagged Src and MBP-tagged RIL. MBP-RIL was coprecipitated with GST-Src (Fig. 2 H, lane 3) but not GST (Fig. 2 H, lane 2), confirming the interaction between the two proteins. To identify Src domains that mediate RIL binding, we generated GST fusion proteins containing the SH3 (residues 88–149), SH2 (residues 150–248), or kinase (residues 249–536) domains of Src. MBP-RIL was coprecipitated with GST kinase domain (Fig. 2 H, lane 5) but not with GST-SH3 (Fig. 2 H, lane 7). A smaller amount of MBP-RIL was also coprecipitated with GST-SH2 (Fig. 2 H, lane 9). Thus, the kinase domain and, to a lesser extent, the SH2 domain but not the SH3 domain mediate the interaction with RIL.

To test whether RIL forms a complex with Src in cells, we immunoprecipitated Flag-RIL from Flag-RIL–expressing HCT116 cells (Fig. 2 I, lane 3). Src was readily coimmunoprecipitated with Flag-RIL (Fig. 2 I, lane 3). In control experiments, no Src was detected in anti-Flag immunoprecipitates derived from control transfectants lacking Flag-RIL (Fig. 2 I, lane 2). To further test this, we immunoprecipitated endogenous RIL from WI-38 cells. Again, Src was readily coimmunoprecipitated with RIL (Fig. 2 J, lane 3). Thus, consistent with the colocalization (Fig. 2, A–C) and direct binding (Fig. 2, G and H) experiments, RIL forms a complex with Src in cells.

The finding that RIL binds Src suggested two potential mechanisms by which RIL could suppress Src activation. First, RIL binding could potentially interfere with conformation changes involved in Src activation and thereby suppresses Src activation. Alternatively, RIL could function as an adapter protein for a protein phosphatase and consequently link the phosphatase to Src and promote pY419 dephosphorylation, resulting in Src inactivation. To test the first possibility, we incubated purified Src with GST-RIL and found that it did not reduce the kinase activity (Fig. 3 A). Thus, RIL binding alone is insufficient for Src inactivation. To test the second possibility, we immunoprecipitated Flag-RIL (Fig. 3 B, lane 2) and analyzed associated phosphatase activity. A significantly higher phosphatase activity was detected in Flag-RIL immunoprecipitates compared with that of the control immunoprecipitates (Fig. 3 C). Deletion of the LIM domain or the second zinc finger within the LIM domain significantly reduced the phosphatase activity (Fig. 3 D).

What is the molecular identity of the phosphatase involved in RIL-mediated Src inactivation? Protein Tyr phosphatase (PTP)–BAS-like (BL), a mouse homologue of human PTPL1, was previously found to interact with RIL (Cuppen et al., 1998), albeit the function of this interaction is unknown. The catalytic sequence of PTPL1 was identified as an Src antagonizer in a functional screen in yeast (Superti-Furga et al., 1996). In vitro, PTP-BL phosphatase domain can catalyze pY419 dephosphorylation (Palmer et al., 2002). Based on these findings, we hypothesized that RIL promotes dephosphorylation of pY419 through recruitment of PTPL1. Up to now, the interaction of PTP-BL with RIL was demonstrated only with recombinant PTP-BL fusion protein. Thus, we sought to test whether RIL forms a complex with endogenous PTPL1 in mammalian cells. The results showed that endogenous PTPL1 was readily coimmunoprecipitated with Flag-RIL (Fig. 3 E, lane 6) but not with control precipitates lacking RIL (Fig. 3 E, lane 5), confirming the interaction of PTPL1 with Flag-RIL in cells.

Next, we sought to test whether PTPL1 binding is required for RIL-induced pY419 dephosphorylation. Deletion of LIM (ΔLIM) or the second zinc finger (ΔZF2) eliminated the PTPL1 binding (Fig. 3 E, lanes 7 and 8). Importantly, expression of the PTPL1 binding–defective ΔLIM (not depicted) or ΔZF2 (Fig. 3 F, lane 3) mutant, unlike that of wild-type RIL (Fig. 3 F, lane 2), failed to inhibit Y419 phosphorylation. These results suggest that the interaction with PTPL1 is required for RIL-mediated dephosphorylation of pY419.

To further test our hypothesis that RIL promotes pY419 dephosphorylation through PTPL1, we depleted PTPL1 by RNAi (Fig. 3, G and H, lanes 3 and 4). Flag-RIL was expressed in PTPL1 knockdown cells (Fig. 3, G and H, lane 3) as well as in control cells expressing a normal level of PTPL1 (Fig. 3, G and H, lane 2). As expected, expression of Flag-RIL substantially reduced Y419 phosphorylation in control cells (Fig. 3, G and H, lane 2). By marked contrast, expression of Flag-RIL failed to inhibit Y419 phosphorylation in the absence of PTPL1 (Fig. 3, G and H, lane 3). Although knockdown of PTPL1 from RIL-expressing cells markedly increased Y419 phosphorylation (Fig. 3, G and H, compare lane 2 with lane 3), the effect of PTPL1 knockdown on Y419 phosphorylation was noticeably diminished in the absence of RIL (Fig. 3, G and H, compare lane 1 with lane 4). Collectively, these results provide strong evidence suggesting that RIL suppresses Src activation by physically linking PTPL1 to Src and consequently promoting pY419 dephosphorylation.

Next, we tested the effect of Src inactivation on RIL binding. Treatment of Src with PP2, a pyrazolo pyrimidine-type inhibitor that is known to lock Src in an inactive conformation

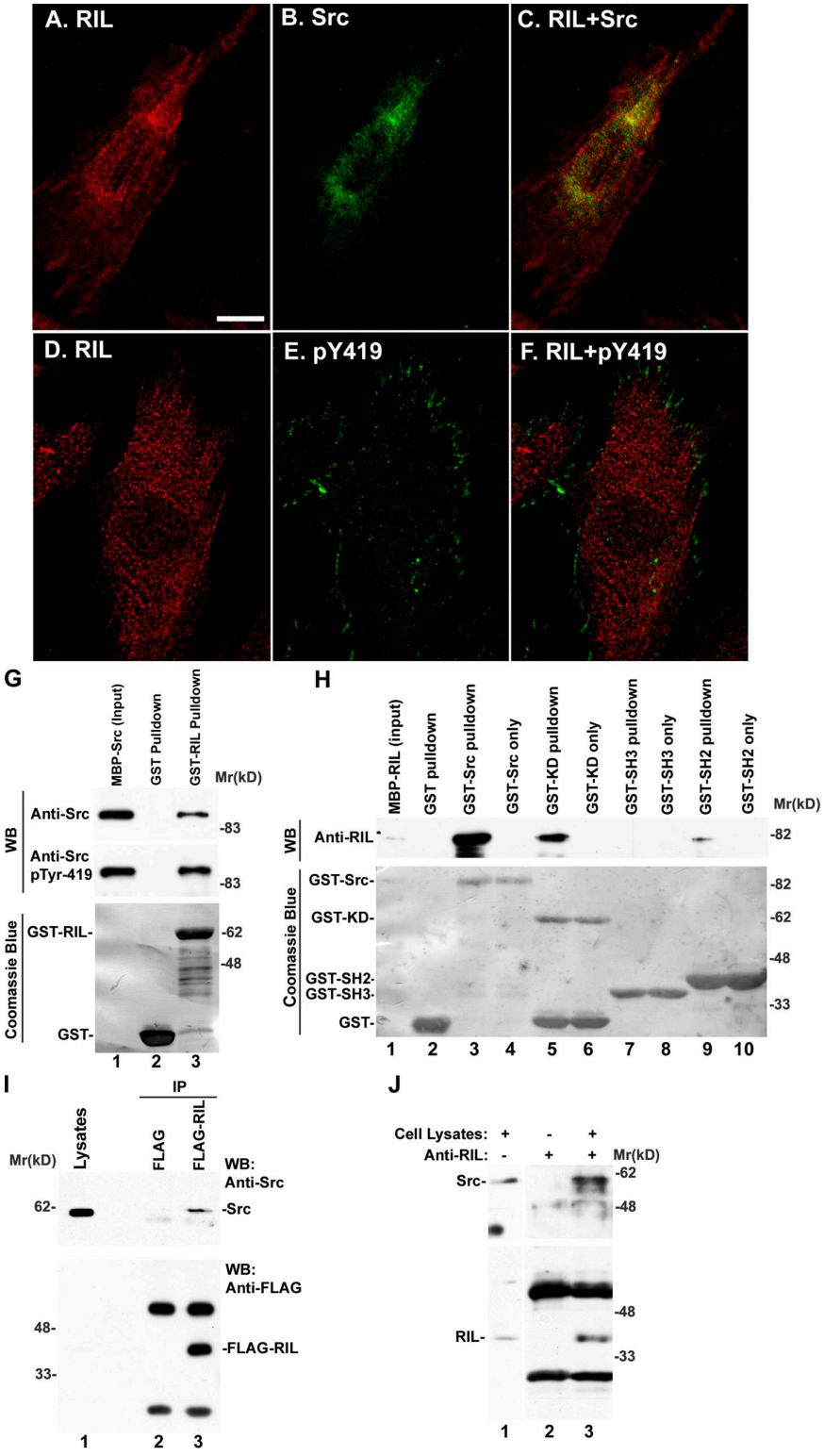

Figure 2. **RIL colocalizes and interacts with Src.** (A–F) WI-38 cells were dually stained with anti-RIL mAb 2A2.11 (A and D) and rabbit anti-Src (B) or anti-pY419 Src (E) antibodies. C and F show merged images. (G) 312.5 ng MBP-Src was incubated with GST or GST-RIL as indicated. The input (lane 1; 10 ng/lane), GST (lane 2), and GST-RIL (lane 3) pull-downs were analyzed by Western blotting and Coomassie blue staining. (H) 250 ng MBP-RIL was incubated with GST or GST fusion protein containing Src SH3, SH2, or kinase domain (KD) as indicated. The input (lane 1; 2 ng/lane) and GST or GST fusion protein pull-downs (lanes 2–10) were analyzed by Western blotting and Coomassie blue staining. (I) 250 µg of lysates of HCT116 cells transfected with Flag-RIL or the control vector were mixed with 20 µl of M2-conjugated agarose beads. Lane 1 was loaded with 5 µg of the control cell lysates (to show the position of Src). The immunoprecipitates were analyzed by Western blotting with anti-Src or anti-Flag antibodies. (J) Anti-RIL immunoprecipitates were prepared by mixing 500 µg WI-38 cell lysates with 5 µg anti-RIL mAb. The lysates (lane 1; 5 µg/lane) and anti-RIL immunoprecipitates (lane 3) were analyzed by Western blotting with anti-Src or anti-RIL antibodies. The sample in lane 2 was prepared as in lane 3 except the lysates were omitted (to show the IgG bands derived from the anti-RIL antibody used in immunoprecipitation). Mr, molecular mass; WB, Western blot; IP, immunoprecipitation. Bar, 15 µm.

(Schindler et al., 1999), abolished the ability of Src to bind RIL (Fig. 4 A, compare lane 5 with lane 6), suggesting that the interaction between Src and RIL is negatively regulated by Src inactivation. This is consistent with the result of our binding experiments showing that pY419 Src was preferentially pulled down by RIL (Fig. 2 G). To directly test this, we substituted Y419 with Phe, which prevents phosphorylation at the activation loop and thereby inhibits full activation of Src (Kmiecik and Shalloway, 1987; Piwnica-Worms et al., 1987; Ferracini and Brugge, 1990). Again, although wild-type Src readily bound to GST-RIL (Fig. 4 B, lane 4), substitution of Y419 with Phe eliminated the ability of Src to interact with GST-RIL (Fig. 4 B, lane 6). In control experiments, neither Src nor Y419F bound to GST (Fig. 4 B, lanes 3 and 5), confirming the specificity of the

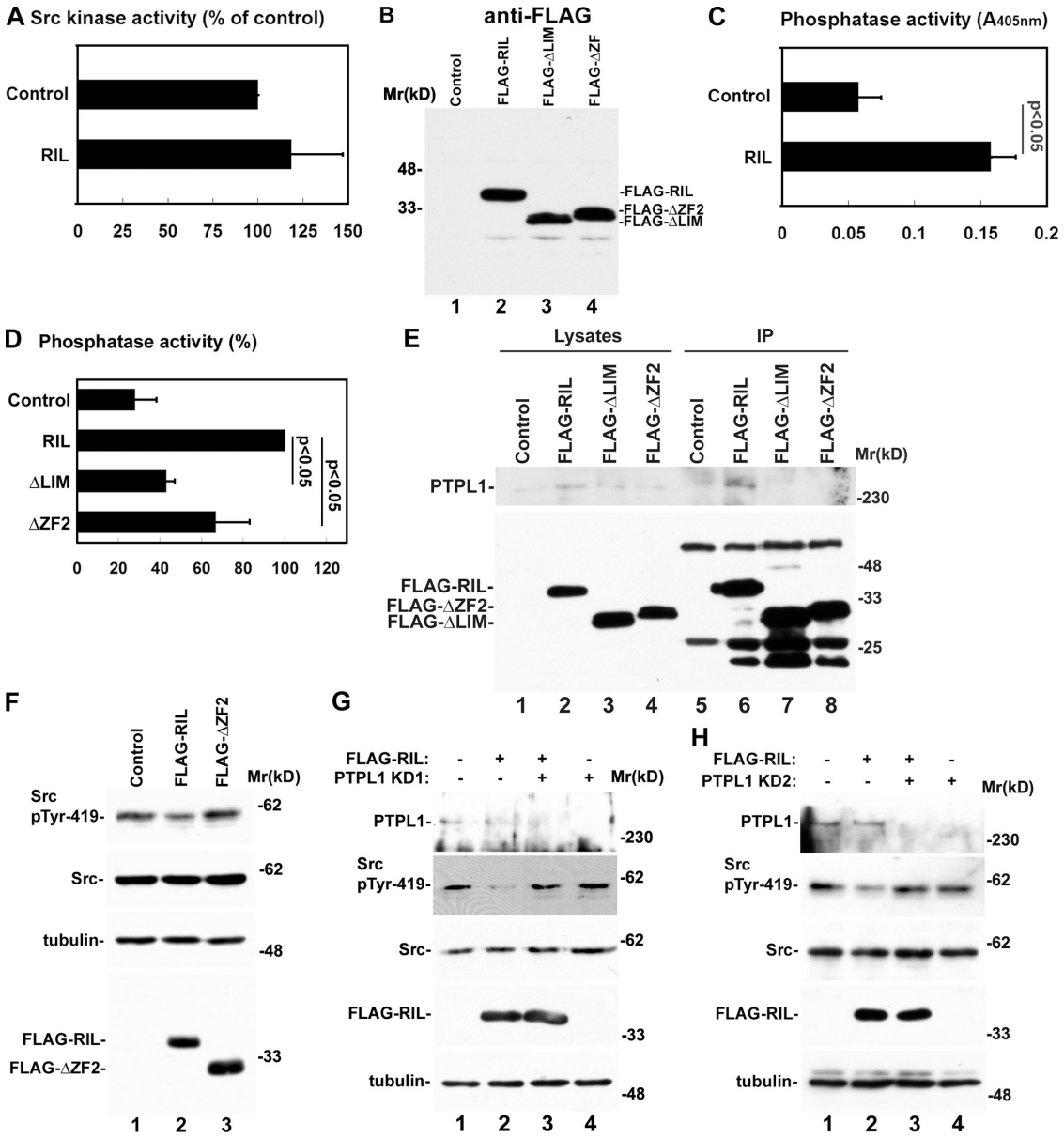

Figure 3. **PTPL1 mediates RIL-induced Src inactivation.** (A) The kinase activity of Src in the presence of GST-RIL was compared with that in the presence of the GST control (normalized to 100%; $n = 2$). (B) Anti-Flag immunoprecipitates were prepared from HCT116 cells transfected with the control vector (lane 1) or vectors encoding Flag-RIL (lane 2), Flag-ΔLIM (lane 3), or Flag-ΔZF2 (lane 4) and analyzed by Western blotting with anti-Flag antibody. (C) Phosphatase activities associated with Flag-RIL and control immunoprecipitates were measured as described in Materials and methods ($n = 4$). (D) Phosphatase activities associated with Flag-ΔLIM, Flag-ΔZF2, or control immunoprecipitates were compared with those associated with Flag-RIL (normalized to 100%; $n = 4$). (E) Anti-Flag immunoprecipitates were prepared by mixing 700 μg cell lysates with 20 μl of M2-conjugated agarose beads. The lysates (lanes 1–4; 15 μg/lane) and immunoprecipitates were analyzed by Western blotting with anti-PTPL1 or anti-Flag antibodies. (F) HCT116 cells were transfected with the control (lane 1), Flag-RIL (lane 2), or Flag-ΔZF2 (lane 3) vector and analyzed by Western blotting with antibodies as indicated. (G and H) HCT116 cells were transfected with the Flag-RIL vector (lanes 2 and 3), the control vector (lanes 1 and 4), control RNA (lanes 1 and 2), and PTPL1 siRNA-1 (G) or -2 (H; lanes 3 and 4) as indicated. The cells were analyzed by Western blotting with antibodies recognizing PTPL1, pY419 Src, Src, Flag, or tubulin. Note that RIL inhibits Y419 phosphorylation in cells that express a normal level of PTPL1 (lane 2) but not in PTPL1 knockdown cells (lane 3). (A, C, and D) Error bars represent mean ± SD. Mr, molecular mass; IP, immunoprecipitate.

binding assay. To further test this, we substituted Pro302 and Pro307 (Pro299 and Pro304 in chickens) in the Y419F mutant with Glu, which is known to convert the Y419F mutant into an active kinase (Gonfloni et al., 2000). The kinase-active Pro302E/Pro307E/Y419F mutant (Fig. 4 C, lane 6), unlike the Y419F kinase-defective mutant (Fig. 4 C, lane 8), was coprecipitated with GST-RIL, confirming that RIL preferentially recognizes active Src. In control experiments, neither Pro302E/Pro307E/Y419F nor Y419F was coprecipitated with GST (Fig. 4 C, lanes 5 and 7). Collectively, our findings suggest a model for RIL-mediated inactivation of Src (Fig. 5). In this model, RIL preferentially recognizes active (i.e., pY419) Src. The binding of RIL to pY419 Src brings it to PTPL1 (Fig. 5 A, step 1), which catalyzes pY419 dephosphorylation. Dephosphorylation of Src at Y419 shifts the balance toward an inactive conformation (similar to the PP2-bound autoinhibited form of Src [Schindler et al., 1999]

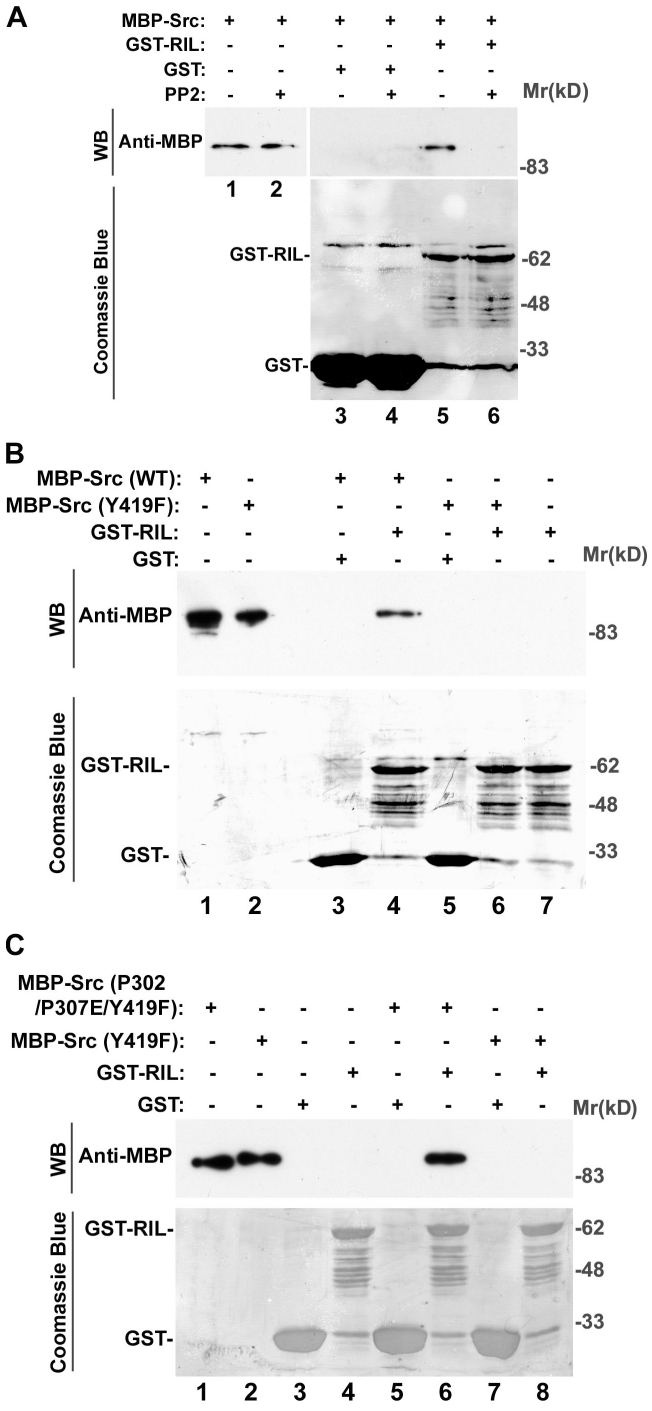

Figure 4. **Inactivation of Src inhibits RIL interaction.** (A) 300 ng MBP-Src was pretreated with (lanes 2, 4, and 6) or without (lanes 1, 3, and 5) PP2 and then incubated with GST-RIL or GST. The inputs (lanes 1 and 2; 5 ng/lane), GST precipitates (lanes 3 and 4), or GST-RIL precipitates (lanes 5 and 6) were analyzed by Western blotting and Coomassie blue staining. (B) 250 ng MBP-Src or 250 ng MBP-Y419F was incubated with GST-RIL or GST. The inputs (lanes 1 and 2; 10 ng/lane), GST precipitates (lanes 3 and 5), or GST-RIL precipitates (lanes 4 and 6) were analyzed by Western blotting and Coomassie blue staining. The sample in lane 7 was prepared as that in lane 4 except that MBP-Src was omitted. (C) 312.5 ng MBP-Y419F or 312.5 ng MBP-Pro302E/Pro307E/Y419F was incubated with GST-RIL or GST as indicated. The inputs (lanes 1 and 2; 10 ng/lane), GST (lanes 5 and 7), or GST-RIL (lanes 6 and 8) precipitates were analyzed by Western blotting and Coomassie blue staining. Lanes 3 and 4 were loaded with GST and GST-RIL pull-downs prepared in the absence of MBP-Y419F or MBP-Pro302E/Pro307E/Y419F. Mr, molecular mass; WB, Western blot.

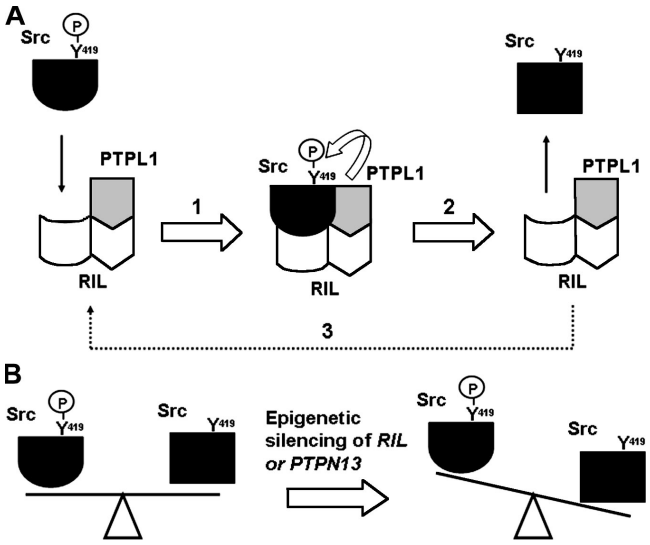

Figure 5. **A model of RIL–PTPL1-mediated Src inactivation.** (A and B) Schematic representations of a RIL–PTPL1-mediated Src inactivation cycle (A) and the effect of loss of RIL or PTPL1 on Src activation (B).

or that of the Y419F mutant), which markedly reduces RIL binding and thus helps to release Src from the RIL–PTPL1 complex (Fig. 5 A, step 2). The free RIL–PTPL1 complex can then bind to another pY419 Src and start a new cycle of pY419 dephosphorylation (Fig. 5 A, step 3). This Src-inactivating cycle counterbalances Src-activating cycles and helps to keep the level of active Src in check in normal cells. Thus, in subcellular compartments in which this RIL-mediated Src inactivation cycle operates, Src activation is suppressed, whereas in areas lacking RIL (e.g., focal adhesions), the level of active Src is elevated. This is highly consistent with our subcellular localization experiments (Fig. 2, A–F) in which high levels of active Src were detected in areas lacking RIL (e.g., focal adhesions) but not in areas where RIL was present. Similarly, in cells (e.g., colon cancer cells) in which RIL is lost as a result of epigenetic silencing, this Src inactivation mechanism is broken, resulting in aberrantly high levels of active (i.e., pY419) Src (Fig. 5 B) and thereby contributing to malignant behavior (e.g., anchorage-independent growth). Our experiments suggest a mechanism through which epigenetic silencing of *RIL* is linked to increased Src activation in colon cancer. Loss of this RIL–PTPL1-mediated Src inactivation cycle in colon cancer cells may provide an explanation as to why vanadate, a phosphatase inhibitor, can activate Src in normal colon cells but not in colon cancer cells (DeSeau et al., 1987). Additionally, our finding that PTPL1 is required for RIL-mediated Src inactivation may explain how epigenetic silencing or genetic mutations in *PTPN13* (the PTPL1 gene), which are frequently found in multiple types of human cancers such as colon cancer (Wang et al., 2004; Yeh et al., 2006; Ying et al., 2006), could contribute to malignant transformation.

In summary, we have demonstrated that RIL functions as an activation-dependent binding protein of Src and mediates a novel Src inactivation cycle. The experiments present in this study shed light on the molecular mechanism underlying aberrant Src activation that has been frequently observed in colon and other human cancers. Given the prominent role of

Src activation in cancer progression, the identification of this RIL-mediated Src inactivation cycle may also help us to develop novel approaches to control cancer progression.

Materials and methods

Cells and antibodies

HCT116 cells were cultured in McCoy's 5A supplemented with L-Gln and 10% FBS. WI-38 cells were cultured with MEM supplemented with 10% FBS and L-Gln. Rabbit polyclonal anti-Src, anti-pY416 Src, anti-pY527 Src, rabbit anti-FAK, and anti-pY566/577-FAK antibodies were purchased from Cell Signaling Technology. A mouse anti-FAK mAb was purchased from BD. Anti-Flag mouse mAb (M2) and M2-conjugated agarose beads were purchased from Sigma-Aldrich. FITC-conjugated anti–mouse IgG and Cy3-conjugated anti–rabbit IgG antibodies were purchased from Jackson ImmunoResearch Laboratories. Alexa Fluor 488–conjugated anti–mouse IgG was purchased from Invitrogen. Mouse mAbs recognizing RIL were prepared using a GST fusion protein containing the N-terminal region of RIL (residues 1–250) as an antigen based on a previously described method (Tu et al., 2003). Hybridoma supernatants were initially screened for anti-RIL activities by ELISA using recombinant MBP-RIL fusion protein. Clones recognizing MBP-RIL in ELISA were selected and further tested by Western blotting using MBP-RIL and mammalian cells expressing Flag-RIL.

Subcellular localization of RIL and Src

Subcellular localization of RIL and Src was analyzed by confocal immunofluorescent staining with mouse anti-RIL and rabbit anti-Src antibodies using a previously described method (Gkretsi et al., 2005). In brief, cells were plated on fibronectin-coated coverslips, fixed with 4% paraformaldehyde, and double stained with mouse anti-RIL and rabbit anti-Src antibodies. The mouse and rabbit antibodies were detected with Cy3-conjugated anti–mouse IgG and Alexa Fluor 488–conjugated anti–rabbit IgG secondary antibodies. The samples were mounted in gelvatol and observed at room temperature under a confocal microscope (FluoView 1000; Olympus) equipped with a 100× NA 1.40 UPLSAPO objective lens. Fluorescence emission was collected with internal photomultiplier tubes and analyzed using FlowView software (Olympus).

RIL expression vector construction, transfection, and immunoprecipitation

The formation of the RIL–Src complex in mammalian cells was analyzed by coimmunoprecipitation. DNA fragments encoding human RIL sequences were cloned into the pFlag-CMV-6c vector (Sigma-Aldrich). HCT116 cells were transfected with the Flag-RIL expression vectors using Lipofectamine Plus (Invitrogen). The expression of Flag-tagged proteins in the transfectants was confirmed by Western blotting and immunofluorescent staining (~70–80% of the transfectants expressed Flag-RIL based on immunofluorescent staining). For immunoprecipitation analyses, the transfectants were lysed with the lysis buffer (1% Triton X-100 in 50 mM Tris-HCl, pH 7.4, containing 150 mM NaCl, 2 mM Na_3VO_4, 25 mM NaF, 1.75% octylglucopyranoside, 0.1 mM PMSF, 1 μM pepstatin, 5 μg/ml aprotinin, and 1 μg/ml leupeptin). The cell lysates were mixed with agarose beads conjugated with anti-Flag mAb M2 (Sigma-Aldrich). To immunoprecipitate endogenous RIL from WI-38 cells, the cell lysates were mixed with anti-RIL mAb 2A2.11 and incubated at 4°C for 4 h. The samples were then incubated with UltraLink Immobilized Protein G (Thermo Fisher Scientific). The beads were washed five times, and the immunoprecipitates were analyzed by Western blotting with antibodies as specified. To prepare anti-FAK immunoprecipitates, HCT116 cells were transfected with the Flag-RIL vector or a Flag vector lacking the RIL sequence as a control. The 750-μg cell lysates were incubated with 1.25 μg anti-FAK mAb. Anti-FAK immunoprecipitates were analyzed by Western blotting with rabbit antibodies specific for FAK or pY566/577 FAK.

RNAi

Two previously validated PTPL1 siRNAs (PTPL1 siRNA-1 [Santa Cruz Biotechnology, Inc.] and -2 [Dromard et al., 2007]) were used to knock down PTPL1. HCT116 cells were transfected with PTPL1 siRNA-1, PTPL1 siRNA-2, or an irrelevant 21-nucleotide RNA using Lipofectamine 2000 reagent (Invitrogen). Depletion of PTPL1 in the PTPL1 siRNA transfectants but not the control transfectants was confirmed by Western blotting with anti-PTPL1 antibody H-300 (Santa Cruz Biotechnology, Inc.).

Direct interaction of RIL with Src

The direct interaction between RIL and Src was analyzed using affinity-purified recombinant GST- or MBP-tagged RIL and MBP- or GST-tagged Src fusion proteins in a GST fusion protein pull-down assay. DNA fragments encoding RIL or Src sequences as specified in each experiment were prepared by PCR and inserted into the pGEX-5x-1 vector (GE Healthcare) or the pMAL-C2 vector (New England Biolabs, Inc.). Point mutations were introduced into the Src coding sequence using a QuikChange Site-Directed Mutagenesis system (Agilent Technologies). The recombinant vectors were used to transform *Escherichia coli* cells. The expression of the GST and MBP fusion proteins was induced with IPTG, and they were purified by affinity chromatography using glutathione–Sepharose 4B and amylose-agarose, respectively, as we previously described (Tu et al., 2003). To test the interaction between GST-RIL and MBP-Src proteins, glutathione–Sepharose 4B beads containing GST-RIL or GST were preincubated with PBS containing 1% (vol/vol) Triton X-100 and 1 mg/ml BSA. The beads were then incubated with 1 μg/ml of MBP-tagged wild-type or mutant forms of Src at 4°C for 2 h and washed five times with 1× PBS/1% Triton X-100. To test the interaction between GST-Src and MBP-RIL proteins, glutathione–Sepharose 4B beads containing GST, GST-tagged wild-type, or mutant forms of Src were preincubated with PBS containing 1% (vol/vol) Triton X-100 and 1 mg/ml BSA and were incubated with MBP-RIL. The samples were analyzed by Western blotting and Coomassie blue staining as specified in each experiment.

Anchorage-independent growth

Anchorage-independent growth was determined using a soft agar colony formation assay as previously described (Kolligs et al., 1999). In brief, HCT116 cells were transfected with the Flag-RIL vector, the Flag-RIL vector and a vector encoding the constitutively active Y527F mutant of chicken Src, or the Flag vector lacking the RIL sequence as a control. 1 d after the transfection, the cells were trypsinized and resuspended in culture medium. Underlayers of 0.6% agar medium were prepared in 12-well plates at 0.5 ml/well by combining equal volumes of 1.2% SeaPlaque agarose (FMC BioProducts) and McCoy's 5A containing 10% FBS. The cells were washed three times with the culture medium and seeded in 12-well plates at 4,000 cells/well in 0.3% SeaPlaque agarose. After incubation at 37°C in 5% CO_2 for 2 wk, colonies with diameters >0.5 mm were counted. The numbers of colonies in each microscopic field (113 mm^2/field) were calculated by analyzing at least six microscopic fields. Colony formation from cells expressing Flag-RIL or Flag-RIL and the constitutively active Src was compared with that of the control cells (presented as percentages of the control cells). The effect of PP2 on anchorage-independent growth was analyzed using the aforementioned protocol except that HCT116 cells were grown in the presence of 10 μM PP2, 10 μM PP3 (a PP2 analogue that lacks Src inhibitory activity), or neither PP2 nor PP3 (control). Colony formation from cells grown in the presence of PP2 or PP3 was compared with that of the control cells (presented as percentages of the control cells).

Src phosphorylation

pY419 or pY530 Src was detected by Western blotting with antibodies specific for the corresponding forms of Src. The densities of pY419 or pY530 Src were quantified by densitometry analysis using the Scion Image program (National Institutes of Health).

Src kinase assays

The effect of RIL binding on Src kinase activity was analyzed using an HTScan(r) Src Kinase Assay kit (Cell Signaling Technology) according to the manufacturer's protocol. In brief, 2 ng/μl GST-Src was incubated with GST-RIL or GST at room temperature for 30 min. The samples were incubated with the substrate peptide for 30 min and mixed with an equal volume of 50 mM EDTA to stop the reaction. The reaction solutions were transferred into 96-well streptavidin plates (Millipore) at 25 μl/well, diluted with 75 μl H_2O, and incubated at room temperature for 60 min. At the end of the incubation, the wells were rinsed three times with 0.1% Triton X-100 in PBS and incubated with anti–phospho-Tyr antibody pY-100 (1:1,000 dilution) for 60 min. After washing three times with 0.1% Triton X-100 in PBS, the wells were incubated with HRP-conjugated goat anti–mouse IgG antibody (1:1,000 dilution) for 60 min. The wells were rinsed six times with 0.1% Triton X-100 in PBS, 100 μl of 1 mg/ml TMB (3,3′,5,5′-tetramethylbenzidine dihydrochloride; Electron Microscopy Sciences) was added to each well, and they were incubated for 15 min. The reaction was stopped by adding 100 μl 2N H_2SO_4 to each well. Absorbance at 450 nm was read using a microplate reader (GENios; Tecan). For Src immunoprecipitation kinase assay, the lysates of HCT116 cells transfected with the control or Flag-RIL vector were incubated with rabbit anti-Src antibody at 4°C for 60 min followed by incubation with protein A/G–agarose beads (Santa Cruz Biotechnology, Inc.) for 30 min. The kinase activities of Src immunoprecipitates were analyzed as described above.

Phosphatase assay

Phosphatase activities associated with RIL were analyzed using *p*-nitrophenyl phosphate as a substrate in an immune complex phosphatase assay as described previously (Pazdrak et al., 1997). In brief, HCT116 cells were transfected with vectors encoding Flag-tagged wild-type or mutant forms of RIL or Flag vector lacking the RIL sequence as a control. 1 d after the transfection, the cells were lysed in the lysis buffer (1% Triton X-100 in 50 mM Tris-HCl, pH 7.4, containing 150 mM NaCl, 25 mM NaF, 1.75% octylglucopyranoside, 0.1 mM PMSF, 1 µM pepstatin, 5 µg/ml aprotinin, and 1 µg/ml leupeptin) and incubated with 30 µl of anti-Flag antibody (M2)–conjugated beads at 4°C for 3 h. The beads were washed three times with the lysis buffer and three times with the phosphatase buffer (50 mM Hepes, pH 7.2, 60 mM NaCl, 50 mM KCl, 0.1 mM PMSF, 1 µM pepstatin, 5 µg/ml aprotinin, and 1 µg/ml leupeptin). Each sample of the RIL immunoprecipitates or the control immunoprecipitates was incubated with 100 µl of 5 mM *p*-nitrophenyl phosphate in phosphatase buffer containing 1 mg/ml BSA, 10 mM DTT, and 5 mM EDTA at 30°C. Absorbance at 405 nm was read using a GENios microplate reader.

Statistical analysis

Statistical analysis was performed using the Student's *t* test. A p-value of <0.05 was considered to be statistically significant and is indicated in the figures.

We thank Dr. Donna B. Stolz for assistance in confocal imaging.

This work was supported by National Institutes of Health grants GM65188 and DK54639 to C. Wu.

Submitted: 24 October 2008
Accepted: 18 February 2009

References

Aligayer, H., D.D. Boyd, M.M. Heiss, E.K. Abdalla, S.A. Curley, and G.E. Gallick. 2002. Activation of Src kinase in primary colorectal carcinoma: an indicator of poor clinical prognosis. *Cancer*. 94:344–351.

Bolen, J.B., A. Veillette, A.M. Schwartz, V. DeSeau, and N. Rosen. 1987. Activation of pp60c-src protein kinase activity in human colon carcinoma. *Proc. Natl. Acad. Sci. USA*. 84:2251–2255.

Boumber, Y.A., Y. Kondo, X. Chen, L. Shen, V. Gharibyan, K. Konishi, E. Estey, H. Kantarjian, G. Garcia-Manero, and J.P. Issa. 2007. RIL, a LIM gene on 5q31, is silenced by methylation in cancer and sensitizes cancer cells to apoptosis. *Cancer Res.* 67:1997–2005.

Cartwright, C.A., M.P. Kamps, A.I. Meisler, J.M. Pipas, and W. Eckhart. 1989. pp60c-src activation in human colon carcinoma. *J. Clin. Invest.* 83:2025–2033.

Cartwright, C.A., A.I. Meisler, and W. Eckhart. 1990. Activation of the pp60c-src protein kinase is an early event in colonic carcinogenesis. *Proc. Natl. Acad. Sci. USA*. 87:558–562.

Cuppen, E., H. Gerrits, B. Pepers, B. Wieringa, and W. Hendriks. 1998. PDZ motifs in PTP-BL and RIL bind to internal protein segments in the LIM domain protein RIL. *Mol. Biol. Cell*. 9:671–683.

DeSeau, V., N. Rosen, and J.B. Bolen. 1987. Analysis of pp60c-src tyrosine kinase activity and phosphotyrosyl phosphatase activity in human colon carcinoma and normal human colon mucosal cells. *J. Cell. Biochem.* 35:113–128.

Dromard, M., G. Bompard, M. Glondu-Lassis, C. Puech, D. Chalbos, and G. Freiss. 2007. The putative tumor suppressor gene PTPN13/PTPL1 induces apoptosis through insulin receptor substrate-1 dephosphorylation. *Cancer Res.* 67:6806–6813.

Ferracini, R., and J. Brugge. 1990. Analysis of mutant forms of the c-src gene product containing a phenylalanine substitution for tyrosine 416. *Oncogene Res.* 5:205–219.

Frame, M.C. 2004. Newest findings on the oldest oncogene; how activated src does it. *J. Cell Sci.* 117:989–998.

Gkretsi, V., Y. Zhang, Y. Tu, K. Chen, D.B. Stolz, Y. Yang, S.C. Watkins, and C. Wu. 2005. Physical and functional association of migfilin with cell-cell adhesions. *J. Cell Sci.* 118:697–710.

Gonfloni, S., A. Weijland, J. Kretzschmar, and G. Superti-Furga. 2000. Crosstalk between the catalytic and regulatory domains allows bidirectional regulation of Src. *Nat. Struct. Mol. Biol.* 7:281–286.

Kiess, M., B. Scharm, A. Aguzzi, A. Hajnal, R. Klemenz, I. Schwarte-Waldhoff, and R. Schafer. 1995. Expression of ril, a novel LIM domain gene, is down-regulated in Hras-transformed cells and restored in phenotypic revertants. *Oncogene*. 10:61–68.

Kmiecik, T.E., and D. Shalloway. 1987. Activation and suppression of pp60c-src transforming ability by mutation of its primary sites of tyrosine phosphorylation. *Cell*. 49:65–73.

Kolligs, F.T., G. Hu, C.V. Dang, and E.R. Fearon. 1999. Neoplastic transformation of RK3E by mutant beta-catenin requires deregulation of Tcf/Lef transcription but not activation of c-myc expression. *Mol. Cell. Biol.* 19:5696–5706.

Kopetz, S., A.N. Shah, and G.E. Gallick. 2007. Src continues aging: current and future clinical directions. *Clin. Cancer Res.* 13:7232–7236.

Palmer, A., M. Zimmer, K.S. Erdmann, V. Eulenburg, A. Porthin, R. Heumann, U. Deutsch, and R. Klein. 2002. EphrinB phosphorylation and reverse signaling: regulation by Src kinases and PTP-BL phosphatase. *Mol. Cell*. 9:725–737.

Pazdrak, K., T. Adachi, and R. Alam. 1997. Src homology 2 protein tyrosine phosphatase (SHPTP2)/Src homology 2 phosphatase 2 (SHP2) tyrosine phosphatase is a positive regulator of the interleukin 5 receptor signal transduction pathways leading to the prolongation of eosinophil survival. *J. Exp. Med.* 186:561–568.

Piwnica-Worms, H., K.B. Saunders, T.M. Roberts, A.E. Smith, and S.H. Cheng. 1987. Tyrosine phosphorylation regulates the biochemical and biological properties of pp60c-src. *Cell*. 49:75–82.

Playford, M.P., and M.D. Schaller. 2004. The interplay between Src and integrins in normal and tumor biology. *Oncogene*. 23:7928–7946.

Rosen, N., J.B. Bolen, A.M. Schwartz, P. Cohen, V. DeSeau, and M.A. Israel. 1986. Analysis of pp60c-src protein kinase activity in human tumor cell lines and tissues. *J. Biol. Chem.* 261:13754–13759.

Roskoski, R. Jr. 2005. Src kinase regulation by phosphorylation and dephosphorylation. *Biochem. Biophys. Res. Commun.* 331:1–14.

Russello, S.V., and S.K. Shore. 2004. SRC in human carcinogenesis. *Front. Biosci.* 9:139–144.

Schindler, T., F. Sicheri, A. Pico, A. Gazit, A. Levitzki, and J. Kuriyan. 1999. Crystal structure of Hck in complex with a Src family-selective tyrosine kinase inhibitor. *Mol. Cell*. 3:639–648.

Summy, J.M., and G.E. Gallick. 2003. Src family kinases in tumor progression and metastasis. *Cancer Metastasis Rev.* 22:337–358.

Summy, J.M., and G.E. Gallick. 2006. Treatment for advanced tumors: Src reclaims center stage. *Clin. Cancer Res.* 12:1398–1401.

Superti-Furga, G., K. Jonsson, and S.A. Courtneidge. 1996. A functional screen in yeast for regulators and antagonizers of heterologous protein tyrosine kinases. *Nat. Biotechnol.* 14:600–605.

Thomas, S.M., and J.S. Brugge. 1997. Cellular functions regulated by Src family kinases. *Annu. Rev. Cell Dev. Biol.* 13:513–609.

Tu, Y., S. Wu, X. Shi, K. Chen, and C. Wu. 2003. Migfilin and mig-2 link focal adhesions to filamin and the actin cytoskeleton and function in cell shape modulation. *Cell*. 113:37–47.

Wang, Z., D. Shen, D.W. Parsons, A. Bardelli, J. Sager, S. Szabo, J. Ptak, N. Silliman, B.A. Peters, M.S. van der Heijden, et al. 2004. Mutational analysis of the tyrosine phosphatome in colorectal cancers. *Science*. 304:1164–1166.

Yeatman, T.J. 2004. A renaissance for SRC. *Nat. Rev. Cancer*. 4:470–480.

Yeh, S.H., D.C. Wu, C.Y. Tsai, T.J. Kuo, W.C. Yu, Y.S. Chang, C.L. Chen, C.F. Chang, D.S. Chen, and P.J. Chen. 2006. Genetic characterization of fas-associated phosphatase-1 as a putative tumor suppressor gene on chromosome 4q21.3 in hepatocellular carcinoma. *Clin. Cancer Res.* 12:1097–1108.

Ying, J., H. Li, Y. Cui, A.H. Wong, C. Langford, and Q. Tao. 2006. Epigenetic disruption of two proapoptotic genes MAPK10/JNK3 and PTPN13/FAP-1 in multiple lymphomas and carcinomas through hypermethylation of a common bidirectional promoter. *Leukemia*. 20:1173–1175.